MOL # 117515

Comparative docking to distinct G protein-coupled receptor conformations exclusively yields ligands with agonist efficacy

Magdalena M. Scharf[a], Moritz Bünemann[b], Jillian G. Baker[c], and Peter Kolb[a]

[a]Institute of Pharmaceutical Chemistry, Philipps-University Marburg, Marbacher Weg 6, 35032 Marburg, Germany

[b]Institute of Pharmacology and Clinical Pharmacy, Philipps-University Marburg, Karl-von-Frisch-Straße 2, 35043 Marburg, Germany

[c]Cell Signalling, School of Life Science, Queen's Medical Center, University of Nottingham, Nottingham NG7 2UH, United Kingdom

Running Title Page

Running Title: GPCR active conformation docking to find agonists

Corresponding authors:

Dr Peter Kolb, Institute of Pharmaceutical Chemistry, Philipps-University Marburg, Marbacher Weg 6, 35032 Marburg, Germany; Tel. +49 6421 28 25908; Fax: +49 6421 28 28994; Email: peter.kolb@uni-marburg.de

Dr Jillian G. Baker, Cell Signalling, School of Life Science, Queen's Medical Center, University of Nottingham, Nottingham NG7 2UH, United Kingdom; Tel. +44 115 82 30085; Fax: +44 115 82 30081; Email: jillian.baker@nottingham.ac.uk

Document Statistics:

Text pages: 29

Figures: 5

Tables: 2

Words in abstract: 145

Words in introduction: 569

Words in discussion: 1570

References: 37

Non-standard abbreviations: CHO Chinese hamster ovary; CRE cAMP response element; SPAP secreted placental alkaline phosphatase; DMEM Dulbecco's modified Eagle's medium; ECFP Extended-Connecivity Fingerprints; ECL2 Extracellular loop 2; GPCR G protein-coupled receptor; HEK Human embryonic kidney; PDB Protein Data Bank; ROC Receiver operating characteristic; SAR Structure activity relationship; TM Transmembrane domain; β_1AR Beta-1-adrenergic receptor; β_2AR Beta-2-adrenergic receptor.

List of changes

Abstract

G protein-coupled receptors exist in a whole spectrum of conformations which are stabilised by the binding of ligands with different efficacy or intracellular effector proteins. Here, we investigate whether three-dimensional structures of receptor conformations in different states of activation can be utilised to enrich ligands with agonist behaviour in prospective docking calculations. We focused on the β_2-adrenergic receptor, as it currently is the receptor with the highest number of active-state crystal structures. Comparative docking calculations to distinct conformations of the receptor were used for the *in silico* prediction of ligands with agonist efficacy. The pharmacology of molecules selected based on these predictions was characterised experimentally, resulting in a hit rate of 37% ligands, all of which were agonists. The ligands furthermore contain a pyrazole moiety which has previously not been described for β_2-adrenergic receptor ligands and one of them shows an intrinsic efficacy comparable to salbutamol.

Significance statement

Structure-based ligand design for G protein-coupled receptors crucially depends on receptor conformation and hence their activation state. We explored the influence of using multiple active-conformation X-ray structures on the hit rate of docking calculations to find novel agonists and how to predict the most fruitful strategy to apply. The results suggest that aggregating the ranks of molecules across docking calculations to more than one active-state structure exclusively yields agonists.

Introduction

G protein-coupled receptors (GPCRs) are highly flexible signal transduction proteins that are embedded in the outer membranes of eucaryotic cells. Structurally, they are relatively loose bundles of seven transmembrane (TM) domains that exist in a spectrum of different conformations. (Latorraca et al., 2017) Binding of molecules that enhance signalling, i.e. agonists, to the orthosteric binding pocket (that is located within the transmembrane core for family A GPCRs) shifts the equilibrium between the various conformations such that binding of intracellular effector proteins (e.g. G proteins or arrestins) becomes more likely than in the basal state of the receptor. The receptor thus becomes "activated", and – depending on the effector – a signalling cascade is induced.

At a structural level, the various existing X-ray structures have shown that active conformations are characterised by an outward movement of the intracellular halves of TM V and VI relative to the basal state. This is accompanied by a comparatively small contraction of the orthosteric binding pocket. (Rasmussen et al., 2011) However, whilst binding of an agonist makes receptor-effector coupling more likely, there is also evidence that G protein binding increases the affinity of the receptor for agonists. (De Lean et al., 1980) Recently, a "reverse pharmacology" study demonstrated that extracellular agonists preferentially bind to active receptor conformations. (Pardon et al., 2018) In this study, the β_2-adrenoceptor (β_2AR) was "locked" in an active or inactive conformation through fusion with a G protein-mimicking (Nb80) or an irrelevant (Nbirr) nanobody, respectively. Agonists bound with higher affinity to the "active" β_2AR-Nb80 fusion than to the "inactive" β_2AR-Nbirr receptor fusion. For inverse agonists the opposite binding preference was detected. Furthermore, those ligands that displayed higher affinity for the "active" conformation were confirmed to act as agonists in subsequent cellular assays. Thus, it was possible to predict ligand efficacy from the relative affinity to the two receptor-nanobody constructs, which correspond to different conformational ensembles.

Here, we reproduced the nanobody study *in silico*. It has been shown earlier that such comparative docking calculations can increase the chance of finding molecules with agonist properties in large compound libraries . (Weiss et al., 2013) At the same time, we have demonstrated that already small changes in receptor structure lead to completely different ligand sets. (Kolb et al., 2012). The question thus remained whether

the additional structures of the β_2AR in active conformations that have become available in the past decade would contain novel information and lead to different agonists. Moreover, we investigated what the best way of aggregating the results of multiple docking calculations was. All molecules emerging from the screen were characterised pharmacologically. In order to investigate the selectivity of the ligands' interactions, we performed all experiments on both the β_2AR and the β_1AR.

We here present the results of this study, which did not only have a remarkable overall ligand hit rate of 37 %, but all hits were agonists. Of note, several of the newly discovered ligands feature a pyrazole moiety that has never been described for ligands of the β_2AR before. Somewhat in contrast to earlier work (Weiss et al., 2013) and the nanobody-based assay (Pardon et al., 2018), we found that the comparison of ligand ranks between active and inactive conformations did not lead to the highest enrichment of agonists. We therefore analysed the retrospective enrichments of known β_2AR ligands in the various conformations in order to determine whether this behaviour can be predicted, thus allowing for appropriate choices in prospective screens.

Materials and Methods

Primary docking screen.   The crystal structures with PDB IDs 3SN6 (Rasmussen et al., 2011), 4LDL (Ring

et al., 2013) and 3NY9 (Wacker et al., 2010) were prepared for docking by protonation and subsequent min-

imisation of all hydrogen atoms with CHARMM and the CHARMm22 force field (Momany and Rone, 1992).

In addition, the binding pocket of the 3SN6 structure was relaxed by energy-minimising residues $W109^{3.28}$

(numbers in superscript are according to the Ballesteros-Weinstein enumeration scheme (Ballesteros and

Weinstein, 1995)), $T110^{3.29}$, $D113^{3.32}$, $V117^{3.36}$, $F193^{45.52}$, $N293^{6.55}$ and $N312^{7.39}$ in presence of the ligand

visible in the crystal structure (BI-167107) to ameliorate clashes between ligand and protein, while ensur-

ing that the polar hydrogen atoms of $S207^{5.46}$ and $N293^{6.55}$ were pointing towards the bound ligand, thus

enabling the residues to act as hydrogen bond donors. The spheres that are used in DOCK to translate

and rotate molecules into the binding pocket were moved in order to optimise the enrichment of a set of

124 enantiomers of known β_2AR ligands over decoys generated with DUD-E. (Mysinger et al., 2012) Af-

ter this optimisation step, the *leads now* subset of the ZINC12 library (3,687,621 molecules) (Irwin et al.,

2012) was docked to both crystal structures of the β_2AR in active conformations (PDB IDs 3SN6 and 4LDL;

β_2AR$^{\text{active}}$) using DOCK3.6. (Kuntz et al., 1982; Meng et al., 1992; Shoichet and Kuntz, 1993; Shoichet et al.,

1999; Mysinger and Shoichet, 2010) Besides the individual ranked lists (lists 1 and 3, Fig. 1) determined for

each docking calculation, we also generated another ranked list from the two β_2AR$^{\text{active}}$ dockings in order to

enrich molecules that ranked highly in the docking calculations to *both* structures ("dual reranking", list 2 in

Fig. 1). Furthermore, the rank-ordered list of the docking to the β_2AR$^{\text{active}}$ structure 3SN6 was compared to

the list of a docking to a structure of the β_2AR in an inactive conformation (PDB ID 3NY9; β_2AR$^{\text{inactive}}$)

to identify molecules ranked highly in an active conformation, but poorly in the inactive conformation used

in this study ("selective reranking", list 4 in Fig. 1). Evaluation of the top 500 molecule poses in each of

the four lists (4LDL-based, 3SN6-based, dual reranking, selective reranking) was done visually in order to

manually remove molecules with artificially inflated scores due to any one of the known deficiencies of scoring

functions. (Kolb et al., 2012) For molecules that showed favourable poses but were too big to fit the binding

pocket, smaller derivatives were searched in ZINC12 and docked to 3SN6. A docking calculation to the

$\beta_2 AR^{inactive}$ structure PDB ID 2RH1 (Cherezov et al., 2007) was performed to compare with our previous docking study. (Kolb et al., 2009) This protein structure was prepared and the docking calculation conducted in the same manner as described above. The molecules with the highest numbers of favourable interactions in their poses from all considered ranking lists were pooled and the final list of molecules selected (for IDs and vendors see Supplemental Table 1).

Reranking. Two ranking lists containing the same molecules docked to two different receptor structures were compared with each other to find the highest-ranking molecules from two (dual reranking) lists or those that ranked highly in one, but poorly in the other (selective reranking). Dual reranking was done as described previously. (Schmidt et al., 2015) Briefly, a relative rank R_{rel} for each molecule is calculated for both ranking lists using the rank r of each molecule and the total number of molecules m in the list:

$$R_{rel,i} = \frac{r_i - 1}{m_i - 1} \tag{1}$$

where i is the indicator of each docking. With these relative ranks, a new score D is calculated for each molecule:

$$D = \frac{(R_{rel,1} - R_{rel,2})^2 + R_{rel,1} + R_{rel,2}}{2} \tag{2}$$

Molecules are then ranked according to the new score D. For further explanation on calculations see (Schmidt et al., 2015). Dual reranking was applied to compare the docking calculations to the two structures in an active conformation, i.e. PDB IDs 3SN6 and 4LDL.

For the selective reranking, the new score S was simply calculated as the ratio of the two ranks in the individual dockings:

$$S = \frac{r_2}{r_1} \tag{3}$$

where r_1 is the molecule rank in the list of the docking calculation against 3SN6 and r_2 the molecule rank in the list of the docking calculation against 3NY9.

Similarity-based search for derivatives and structure-based evaluation. Molecules similar to ligands causing the highest accumulation of cAMP in the primary cellular assay were searched in a library of 5,626,190 molecules from ZINC15 (Sterling and Irwin, 2015) using the ECFP4 fingerprint and a Tanimoto

coefficient cutoff of ≥ 0.5. The resulting set of molecules was then docked to the structure with PDB ID

3SN6 using DOCK3.6 and molecules were selected to be tested experimentally after visual inspection of the

molecule poses as described for the primary screen (IDs and Vendors in Supplemental Table 1).

Evaluation of compound novelty.   All molecules that have been tested in any way against the β_2AR were

downloaded from ChEMBL (Gaulton et al., 2012) and filtered for active molecules (2374 unique entries). All

molecules that were tested within the present screen were then compared to this ChEMBL-derived dataset by

their Tanimoto similarity using ECFP4 fingerprints. (Wawer and Bajorath, 2010) To evaluate the similarity

of our ligands to *any* adrenergic receptor, a second dataset was prepared by downloading the bioactivity

data of all molecules targeting any one of the human adrenergic receptors from ChEMBL and filtering it for

actives (7396 unique entries). The similarity evaluation was again done using ECFP4 fingerprints and the

Tanimoto coefficent.

Cell culture.   Stable cell lines of CHO cells expressing either the β_2AR or β_1AR and the CRE-SPAP

reporter gene were grown in Dulbecco's modified Eagle's medium nutrient mix F12 (DMEM/F12) containing

10% fetal calf serum and 2 mM L-glutamine at 37°C in humidified 5% CO_2:95% air atmosphere.

[3]H-CGP 12177 whole cell binding.   Cells were plated to white 96-well plates and grown to conflu-

ence over night. Medium was then removed from the cells and replaced by 100 μL serum-free media (sfm,

DMEM/F12 containing 2 mM L-glutamine) or compound (at twice the final concentration in sfm), followed

immediately by the addition of 100 μL ^{3}H-CGP 12177 in sfm (1:2 dilution in wells). The cells were then incu-

bated at 37°C in humidified 5% CO_2:95% air atmosphere for 2 h. After 2 h, everything was removed from all

wells and the cells were washed twice with 200 μL 4°C phosphate-buffered saline. Microscint 20 (100 μL) was

added to each well and the plates were left at room temperature in the dark for several hours before being

counted on a TopCount. (Baker, 2005) Propranolol (10 μM) was used to define non-specific binding in all

plates and the final concentration of ^{3}H-CGP 12177 was 0.5-0.9 nM. All compounds were examined in 7-point

concentration response curves with each condition repeated in triplicate in each experiment. A sigmoidal

curve was fitted to the data using Graphpad Prism 7 and an IC_{50} determined from the following equation.

$$\% \text{ specific binding} = 100 - \frac{100}{1 + 10^{(log(\text{IC}_{50}) - log[\text{A}])}} \qquad (4)$$

where [A] is the concentration of the competing ligand and IC_{50} is the concentration at which half of the specific binding of ^{3}H-CGP 12177 has been inhibited.

From the IC_{50} value and the known concentration of radioligand, [^{3}H-CGP 12177], a K_D value (concentration at which half the receptors are bound) was calculated using the Cheng–Prusoff equation:

$$\text{K}_D = \frac{\text{IC}_{50}}{1 + \frac{[^3H - CGP\,12177]}{\text{K}_D(^3H - CGP\,12177)}} \qquad (5)$$

The K_D of ^{3}H-CGP 12177 in these cells was 0.42 nM for the β_1AR and 0.17 nM for the β_2AR. (Baker, 2005)

CRE-SPAP production. Cells were plated to clear 96-well plates and grown to confluence overnight. Media was then removed from all wells and replaced with 100 μL sfm for 24 h (i.e. cells were serum starved). The following day, media was again removed and replaced by 100 μL fresh sfm. Where used, antagonists diluted in sfm were used instead of pure sfm. Compound (10 μL diluted in sfm) was then added to the wells and the cells incubated for 5 h at 37°C and humidified 5% CO$_2$:95% air atmosphere. After 5 h, everything was removed from all wells and replaced by 40 μL sfm. Cells were then incubated for 1 h at 37°C and humidified 5% CO$_2$:95% air atmosphere before being placed in a 65°C oven for 30 min. The plates were cooled to room temperature and 100 μL of 5 mM *para*-Nitrophenylphosphate in DEA buffer (1 M diethanolamine, 0.28 M NaCl, 0.5 mM MgCl$_2$, pH 9.85) added to each well. Once the yellow colour had developed, plates were read on an MRX plate reader through a 405 nm filter. (Baker et al., 2014) Isoprenaline (10 μM) was used as a positive control in all plates. All compounds were examined as a 7-point concentration-response with triplicate condition for each concentration of ligand. A sigmoidal concentration response curve was fitted to the data using GraphPad Prism 7 (eq. 6).

$$Response = \frac{\text{E}_{max}}{1 + 10^{(log(\text{EC}_{50}) - log[\text{A}])}} \qquad (6)$$

where E_{max} is the maximum response, [A] is the agonist concentration and EC_{50} is the concentration of agonist that produces 50% of the maximal response.

To prove that the agonist responses were indeed occurring via the transfected βAR, the affinity (log K_D value) of CGP 20712A or ICI 118551 was calculated from the rightward shift of the agonist concentration responses in the presence of a fixed concentration of antagonist using the Gaddum equation:

$$DR = 1 + \frac{[B]}{K_D} \tag{7}$$

where DR (dose ratio) is the ratio of the agonist concentration required to stimulate an identical response in the presence and absence of the fixed concentration of antagonist [B].

Efficacy ratios. As the affinity (K_D) and potency of the agonist response (EC_{50}) for each ligand were determined in the same cell lines and ligands were all examined in parallel experiments, an indicator of intrinsic efficacy (ability of a compound to stimulate a response) can be determined from the efficacy ratio (K_D/EC_{50}) at each receptor. This therefore takes into account the affinity of the ligand, and although the score cannot be compared across cell lines, it can be used to rank ligands in order of intrinsic efficacy at each receptor. Thus cimaterol, with a β_2AR affinity (K_D) of 81 nM and a β_2AR EC_{50} value of 0.21 nM, is very efficacious as it hardly needs to occupy any receptors in order to stimulate a maximum response (efficacy ratio of 386). At the same receptor, salmeterol, although of higher affinity (K_D 0.81 nM, EC_{50} 0.012 nM), once bound, is less efficacious (efficacy ratio 67). CGP 12177 is a partial agonist (as can be seen from the 37% stimulation in relation to isoprenaline). As a partial agonist, it needs to occupy all of the available receptors to stimulate its maximum 37% response, and the K_D value (0.28 nM) and EC_{50} value (0.19 nM) are similar, giving a low efficacy ratio of 1.47.

Results

Primary docking screen.   The *leads now* subset of the ZINC12 library (Irwin et al., 2012) consisting of 3,687,621 molecules was docked to two β_2AR^{active} (PDB IDs 3SN6 and 4LDL)). As described in the Methods, four different schemes were used to rank the molecules from the docking calculations (detailed in Fig. 1). Molecules were ranked individually in both conformations (list 1 [red] and list 3 [yellow] in Fig. 1) and re-ranked to identify consistently favourably ranked molecules (list 2 [orange] in Fig. 1) as well as those that had a large difference in ranks when compared to the docking to a $\beta_2AR^{inactive}$ (PDB ID 3NY9; list 4 [green] in Fig. 1). In each of these four ranking schemes, the top 500 molecules were visually inspected in order to remove molecules that are ranked highly because of insufficient punishment of unfavourable interactions due to the known deficiences of current force fields. From the first three rankings (docking calculations to the β_2AR^{active}; lists 1, 2, and 3 [red, orange, and yellow, respectively] in Fig. 1), 18 molecules were selected and purchased for testing. Five additional molecules showed favourable poses in the orthosteric pocket, but had several parts protruding beyond it, and these parts consequently did not entertain favourable interactions. Smaller derivatives of these molecules were therefore searched in ZINC12, with the aim to keep the key interacting parts constant and only changing the bulky non-interacting moieties. The nine resulting derivative molecules were docked to the 3SN6 structure, poses were evaluated visually and three of the smaller derivatives were selected to be tested (pink box, Fig. 1). The parent molecules of these three derivatives emerged from the dual reranking (3SN6 vs. 4LDL; one derivative) and the selective reranking (3SN6 vs. 3NY9; two derivatives), respectively. Interestingly, ranking 4, contrasting the results from a docking calculation to a $\beta_2AR^{inactive}$ and a β_2AR^{active}, did not yield any molecules that were deemed worth testing after visual inspection.

One additional molecule was selected from a separate docking calculation to the $\beta_2AR^{inactive}$ structure with PDB ID 2RH1 (list 6 [darker blue] in Fig. 1), which we had done to compare with our earlier study. (Kolb et al., 2009) Molecule **8** was chosen because of its pose in the $\beta_2AR^{inactive}$, which featured interactions with D113[3.32]. Interestingly, this molecules did not feature the same docking pose in the various β_2AR^{active} docking calculations because the bulky substituent of **8** forced a flipped pose in the pocket. Nonetheless, we decided to evaluate it as a possible agonist because of its significantly smaller size, which is generally considered to

be one of the hallmarks of β_2AR agonists.

Similarity-based search for derivatives of the initial hits and structure-based evaluation. An initial evaluation of the compounds in a cAMP-accumulation-based assay in HEK293T cells (Results in Supplemental Data, Supplemental Fig. 1) revealed two ligands with a higher-than-average percentage of activation, **1** and **2**. These two molecules are close analogs of each other. A similarity search with these molecules as query retrieved 62 additional molecules. Since the parent molecules had the highest ranks in the docking calculation using β_2AR$^{\text{active}}$ structure 3SN6, the derivatives were docked to the same structure to evaluate their steric fit. A complementary docking to the β_2AR$^{\text{inactive}}$ structure 3NY9 was used to compare the docking poses and validate them. Based on their favourable poses, five molecules were selected for detailed pharmacological analysis (salmon box in Fig. 1).

Pharmacological characterisation. A total of 27 molecules (22 from the primary docking screen and 5 from the similarity-based search) were examined in CHO cells stably expressing either the human β_2AR (CHO-β_2) or the human β_1AR (CHO-β_1).

Ligand affinity was determined from a whole cell ^{3}H-CGP 12177 radioligand displacement assay. CGP 20712A, a known β_1AR-antagonist, bound to the β_2AR with much lower affinity than the β_1AR (log K_D -5.8 and -8.6, respectively), whilst ICI 118551 bound to the β_2AR with higher affinity (log K_D -9.3 at the β_2AR, -6.8 at the β_1AR), thus demonstrating the presence of the two receptors in the respective cell lines (Table 1). Of the 27 ligands examined, ten were found to have measureable affinity, eight from the primary screen and two from the similarity-based search. A further six molecules had very low affinity such that the calculation of K_D values was not possible. The compound with the highest affinity was **1** with an affinity for both the β_2AR and the β_1AR of around 520 nM (Table 1, Fig. 2).

The ability of compounds to stimulate a functional response was then examined in the same cells using the CRE-SPAP reporter stably expressed in both cell lines. The benefit of this system is that it is an amplified downstream readout, thus maximising the chances of detecting any agonist properties. (Baker et al., 2004) Given that partial agonists may be amplified to appear more like full agonists in this system, several well-known partial agonists were included in the study for comparative purposes. Cimaterol, a

relatively nonselective βAR agonist, stimulated a full agonist response with respect to isoprenaline in both cell lines ($\log EC_{50}$ -9.7 at the β_2AR, $\log EC_{50}$ -8.6 at the β_1AR, Table 2). As expected, denopamine, a known β_1AR-selective agonist, stimulated a full agonist response that was more potent in the β_1AR cell line, whilst salbutamol, a known β_2AR-selective agonist, was more potent in the β_2AR cell line (Baker, 2010) (Table 2). As anticipated, the 17 compounds with no affinity in the binding assay were also not able to stimulate any significant agonist response in either cell line. These compounds therefore did not interact with either the β_2AR or β_1AR.

Of the ten compounds that did have measureable affinity, all showed agonist efficacy (Table 2, Fig. 2) and **1** was the most potent ligand at both receptors. However, it was important to be sure that these agonist responses were indeed occurring via the transfected receptors. Dose responses were therefore examined in the parent CHO-CRE-SPAP cells that contain the stably transfected reporter gene but no transfected receptor. No agonist responses were elicited by any of the ten novel agonist compounds, nor by cimaterol, denopamine, salbutamol, salmeterol or CGP 12177, in CHO-CRE-SPAP cells (n=3 for each ligand).

Finally, the agonist responses were inhibited by the selective antagonists CGP 20712A and ICI 118551 in their respective cell lines. In the CHO-β_2 cells, agonist responses to cimaterol, salbutamol, salmeterol, denopamine and CGP 12177 inhibited by ICI 118551 yielded very similar $\log K_D$ values (approximately $\log K_D$ -9.6, and similar to the $\log K_D$ value of ICI 118551 (-9.3) determined from the binding assay, Table 1, 2). Similar high affinity values for ICI 118551 were obtained from its ability to inhibit the agonist responses to the ten novel compounds (Table 2). This suggests that all these ligands were acting via the orthosteric pocket of the transfected β_2AR, its orthosteric pocket and the same receptor conformation. Compound **8** stimulated a partial agonist response in the CHO-β_2 cells, and although it was inhibited by ICI 118551, a right-ward shift and flattening of the curve was observed. As such, the dose-response curve did not reach the same maximum in the presence of ICI 118551 and thus a $\log K_D$ could not be calculated using the Gaddum equation.

The β_1AR exists in at least two conformations: a high-affinity catecholamine conformation (where responses are readily inhibited by antagonists) and a low-affinity secondary conformation (where inhibition of agonist responses requires much higher concentrations of antagonist) where CGP 12177 is an agonist. (Konkar et al., 2000; Granneman, 2001) In the CHO-β_1 cells, agonist responses to cimaterol, salbutamol, salmeterol and

denopamine were inhibited by CGP 20712A to yield high affinity values for CGP 20712A, again similar to those seen from the binding assay (Table 1, 2). The agonist response to CGP 12177, however, required significantly higher concentrations of CGP 20712A to achieve a right-ward shift, and thus yielded a $\log K_D$ value for CGP 20712A much lower than that of the other compounds (Table 2). This is because the agonist response to CGP 12177 is occurring via the secondary conformation. (Baker, 2005) The agonist responses to the novel compounds were all inhibited by CGP 20712A to yield values very similar to those for the literature compounds, and similar to those obtained in the binding assay. All of these compounds are therefore exerting their agonist action through the orthosteric pocket in the primary catecholamine conformation of the β_1AR. Perhaps not surprisingly, as this is the conformation most similar to that of the β_2AR.

Hit rates. In total, we tested 27 molecules, 22 emanating from the primary docking screen and 5 from the similarity-based search. The competition binding assay confirmed 10 new ligands of these 27 tested molecules, corresponding to a hit rate of 37 % (see Table 1, Supplemental Table 2) . All of the 10 compounds showed agonistic activity, i.e. again a 37% overall hit rate or 100% of the discovered ligands (Table 2). Two of these novel agonists resulted from the similarity-based search (i.e. 2 of 5 molecules, a 40% hit rate). Only 1 of the 22 molecules from the primary screen was retrieved from the docking calculation to the inactive receptor 2RH1 (5%). The majority of discovered agonists, 7, originated from the dual reranking (7/22 molecules; 32%). The overall hit rate of 37 % is at the upper end compared to other docking studies using the β_2AR (Sabio et al., 2008; Kolb et al., 2009; Weiss et al., 2013; Schmidt et al., 2017; Chevillard et al., 2019) or related aminergic GPCRs (Carlsson et al., 2011; Kruse et al., 2013).

Correlation between retrospective ligand enrichments and hit rates. The rather large variation in the number of ligands retrieved from the five docking and reranking schemes made us wonder whether this could have been predicted. To that end, we applied the ranking schemes to the set of 124 known active enantiomers and their decoys that had originally been used to optimise the docking procedure. For each of the resulting ranking lists we calculated receiver operating characteristic (ROC) plots. These plots allow assessment of the enrichment of agonists and antagonists in the top ranks versus the decoy molecules in each of the docking schemes. Agonists are enriched to a similar extent in each of the docking calculations

to a β_2AR^{active} as well as in both reranked lists and also better than antagonists (Fig. 3, Supplemental Fig. 2). Furthermore, selective reranking leads to below-random enrichment of antagonists, albeit with an early enrichment similar as in the docking calculations to the two β_2AR^{active} structures.

Interestingly, although overall enrichment of agonists and antagonists in the ranking lists of the dual reranking does not differ noticably from the other three ranking schemes, antagonists are only enriched after roughly 6 % of the decoys have been found. For a set of 3.6 million molecules (such as the one we used here) this would mean that no antagonists appear in the top 200,000 molecules of the dual reranking list and, therefore, all hits from the top 200,000 should be agonists. While this is certainly overestimating the results, this reasoning is in line with the hit rate achieved during the large library docking screen.

Ligand novelty. Novelty of the discovered ligands was evaluated by comparison to all compounds binding to or acting at the β_2AR or any adrenergic receptor according to ChEMBL. (Gaulton et al., 2012) While the most active novel agonist discovered during this screen, compound **1**, is similar to known βAR agonists in that it contains a β-hydroxy-amine, it also contains a pyrazole moiety, a feature it shares with six of the novel agonists discovered in the primary docking screen. Molecules featuring this moiety have so far never been described as ligands of the β_2AR. Because of this unprecedented ring, the ligands have relatively low Tanimoto similarity values compared to known β_2AR ligands in ChEMBL (Gaulton et al., 2012). The highest similarity value was 0.47 (**8** to CHEMBL599896) and only four molecules showed a similarity > 0.4 (see Supplemental Table 3). None of the most similar compounds contained the same structural motifs as the query molecules.

The more general comparison against ligands of *any* adrenergic receptor revealed a similar picture. The highest similarity was 0.49 (low affinity **14** to CHEMBL15303) or 0.47 (**8** to CHEMBL599896) within this search. Matches with a similarity > 0.4 were found for only seven of the molecules (see Supplemental Table 4). Casting an even wider net, all compounds containing the basic substructure of phenyl, β-hydroxy-amine and pyrazole where retrieved from ChEMBL. None of them was associated with bioactivity data for the β_2AR. We note that compound **7** has previously been described as a weak κ-opioid receptor antagonist ($pK_i = 5.19$) (Zheng et al., 2017), but never as a β_2AR ligand. (Wawer and Bajorath, 2010)

Predicted binding poses. In the predicted docking pose, the β-hydroxy-amine of **1** interacts with D113$^{3.32}$ and N312$^{7.39}$ (Fig. 4A). The fluorine substituent in *ortho* position on the aromatic moiety might contribute interactions with the protein (potentially N293$^{6.55}$ or Y308$^{7.35}$ in the β$_2$AR) that explain its affinity and agonistic activity.

Compound **8** stands out from the other tested molecules since it is the only one that was dicovered from a docking calculation to a β$_2$AR^{inactive}. This molecule has a bulkier structure than the other ligands, with an aliphatic chain and an additional aromatic moiety attached to the more standard benzene ring following the β-hydroxy-amine. Of note, besides the weak H-bond acceptor ether oxygen, there is no other possibility to interact with any of the Ser residues in TM V. In the larger binding pocket of the β$_2$AR^{inactive}, compound **8** is predicted to adopt a pose with the alkyl-aromatic moiety pointing towards ECL2 (Fig. 4B). Unexpectedly, this molecule pose could not be reproduced in a docking calculation to the narrower β$_2$AR^{active} binding pocket. It is interesting to mention that this molecule has only slightly lower affinity (1 μM at the β$_2$AR) than the highest-affinity agonist **1**. One potential reason for its counterintuitive binding preference might be that it is only a partial agonist at the β$_2$AR (with a response of 35% that of isoprenaline and very similar to that of CGP 12177 at 37%). As expected for a partial agonist, the efficacy ratio is low. Despite the large difference in affinity of **8** and CGP 12177 (Table 1), once bound, both compounds have a similar ability to activate the receptor (i.e. have similar intrinsic efficacy, as demonstrated by the efficacy ratio). Given that the CRE-SPAP response is an amplified system, (Baker et al., 2004) **8** can be regarded, just as CGP 12177, a weak partial agonist in the overall ranking of efficacy. Molecule poses of all molecules from the docking calculations to at least one of the used structures can be found in the Supplemental PDB files.

Discussion

This study investigated whether comparative docking to active (and inactive) conformations of the $\beta_2 AR$ could preferentially detect novel compounds with βAR agonist activity, rather than just detect antagonist compounds. Moreover, we tried to determine the impact of using multiple $\beta_2 AR^{active}$ structures and how to best aggregate the individual rankings.

Molecule selection based on docking ranks. Since different approaches were used to retrieve potential ligands with agonistic action from the ranked lists of each docking calculation in the present work, we can evaluate each strategy in terms of the number of agonists retrieved. The initial hypothesis was that agonists would be ranked higher in docking calculations against the $\beta_2 AR^{active}$ than the $\beta_2 AR^{inactive}$. This assumption held true in retrospective studies. Somewhat unexpectedly, however, the selective reranking carried out in this work did not yield molecules that we considered worth testing in the prospective docking. Despite this low abundance of favourably interacting compounds, we still chose two smaller derivatives of compounds emerging from this ranking. All additional compounds tested here were either selected from the individual ranked lists of the docking calculations to the two $\beta_2 AR^{active}$ (PDB IDs 3SN6 and 4LDL) or from the dual reranking taking into account the ranked lists of both of these docking calculations (cf. equation 2).

In our hands, this dual reranking resulted not only in a very high hit rate, but also in a high number of favourably interacting molecule poses in general. Our results therefore suggest that the most fruitful approach to retrieve agonists are docking calculations to more than one structure in an active conformation, aggregating the lists to identify those molecules that are ranked highly in both docking calculations. Turning this around, and somewhat in contrast to our initial assumptions, a high agonist hit rate does not require the comparison of docking calculations against $\beta_2 AR^{active}$ and $\beta_2 AR^{inactive}$ structures.

The comparison to the retrospective docking calculations of known $\beta_2 AR$ ligands suggests that our prospective findings are echoed in the relative enrichments of agonists and antagonists over computer-matched decoys and that such retrospective calculations could be used to indicate *a priori* which reranking scheme might work best.

Closer evaluation of the molecule poses in the $\beta_2 AR^{active}$ and the $\beta_2 AR^{inactive}$, respectively, shows that

orientations are similar, but that the molecule poses in the β_2AR^{active} result, on average, in a higher number of favourable interactions between receptor and molecule. We suggest that this fact can be used as an additional criterion during pose evaluation: While poses of agonists obtained from docking calculations to the β_2AR^{active} should be reproducible in terms of general orientation in docking calculations to the $\beta_2AR^{inactive}$ (since the bigger pocket of the $\beta_2AR^{inactive}$ should leave enough space), the interactions can allow differentiation (see Fig. 5 for an overlay of all four used crystal structures).

We note that one agonist with significantly lower efficacy (**8**) from the primary screen was chosen from the ranked list of a docking calculation to the inactive conformation structure 2RH1. The fact that **8** does not find a favorable pose in the β_2AR^{active} while it is a partial agonist leads to the conclusion that in certain cases the discovery of bulky ligands from a docking calculation to the β_2AR^{active} might be hampered by the rigid conformation used during the calculation. A complementary docking calculation to the $\beta_2AR^{inactive}$ can be helpful here but also includes the risk of incorrect predictions, as statistically a favourable rank in the $\beta_2AR^{inactive}$ but not in the β_2AR^{active} would be taken to indicate an antagonist or inverse agonist. That the discovery of this agonist from a $\beta_2AR^{inactive}$ structure is an exception is supported by the fact that none of the ligands discovered in our earlier studies docking to a $\beta_2AR^{inactive}$ were agonists. (Kolb et al., 2009; Schmidt et al., 2017)

Pharmacological evaluation. Of the 27 compounds chosen from the docking screens for pharmacological evaluation, 10/27 (37%) were found to be agonists of the β_2AR, and most also of the β_1AR, which we used to evaluate the selectivity of the compounds. Importantly, all of these responses were demonstrated to occur at the β_2AR and β_1AR, respectively, because all responses were inhibited by selective antagonists and there were no responses in the parent CHO-CRE-SPAP cells without the transfected receptors. As for many agonists, the affinity of these compounds for the β_2AR and β_1AR was relatively low. (Baker, 2010) However, for all compounds that were found to have measureable binding, we found agonist activity, too.

Whilst it is easy to rank ligands in order of the direct measure of affinity, establishing a ligand's intrinsic efficacy is substantially harder, as there is no single direct pharmacological measure of intrinsic efficacy. One simple way to be able to compare the intrinsic efficacy of compounds is to use an efficacy ratio — comparing

the EC_{50} with the K_D for the same compound, when all compounds are examined in parallel under identical conditions. (Baker, 2010) Here it can be seen that cimaterol is the compound with the highest intrinsic efficacy at both receptors (Table 2). As expected, denopamine had higher intrinsic efficacy at the β_1AR than the β_2AR and salbutamol at the β_2AR than the β_1AR. (Baker, 2010) Of the novel agonists, **1** was the compound with the highest intrinsic efficacy at both the β_1AR and β_2AR, followed by **2**. Of note, none of the derivatives from the analogue search was more active than the parent compounds. By the same measure, compound **1**, the most active molecule, has a similar intrinsic efficacy as salmeterol, a long-acting β_2AR-agonist widely used in the treatment of asthma and COPD. Thus, our approach of docking compounds to different active structures in order to find novel compounds with agonism was able to discover novel compounds with sufficient agonism to be potentially clinically useful. However, interestingly, this approach detected compounds of medium efficacy, and not novel compounds with very high efficacy (such as catecholamines, fenoterol, or even cimaterol or salbutamol (Baker, 2010)).

Structure-Activity Relationship.   Several of the agonist compounds (**1-7**, **9**, **11**, **12**) have rather similar chemical structures and sometimes differ only by one substituent. This allows Structure-Activity Relationship (SAR) conclusions to be drawn. Most compounds feature fluorine atoms at different positions on the aromatic moiety closest to the hydroxyl-group of the β-hydroxy-amine. An additional fluorine atom in *para* position (**6** compared to **5**) had essentially no effect on affinity and intrinsic efficacy. In *meta* position, an additional fluorine atom (**1** compared to **2**), however, leads to increased binding affinity. As expected, the potency (EC_{50}) is also increased, leading to an almost unchanged intrinsic efficacy. The strongest effect on the efficacy can be seen for the *ortho* position. Moving the *ortho*-fluorine atom (**1**) to the *para*-position (**12**) had no effect on affinity, but did reduce the efficacy ratio (especially for the β_2AR; from 1.76 to 1.05, Table 2). Exchanging the fluorine for a chlorine in *ortho* position (**3** compared to **4**) results in almost unchanged affinity and pEC_{50} values. Of note, however, this exchange to a chlorine atom results in a higher % maximum response for the β_2AR (79% for **4** to 95% for **3**) while it results in a lower % maximum response for the β_1AR (60% for **4** to 33% for **3**). This increase can likely be explained by the ability of chlorine to form stronger halogen bonds than fluorine. This could result in a stabilisation of a more active conformation of the receptor. Considering

the difference in responses at the β_2AR and the β_1AR, an interaction of the substituent in *ortho* position

with the protein seems likely. The most plausible candidate is Y308$^{7.35}$ in TM VII (distances of 2.5-4 Å

between the *ortho* substituents of the various ligands and the oxygen of the hydroxyl-group of Y308$^{7.35}$ in

the respective energy-minimised docking poses), which is only present in the β_2AR (it is a Phenylalanine in

the β_1AR).

Finally, the comparison of **2** and **14** indicates that removing the hydroxyl group and introducing an ether in

the alkylic chain between aromatic moiety and secondary amine results in abolishment of binding.

In summary, multi-conformation docking screens appear as a productive strategy to identify novel molecules

with agonism similar to that of clinically used drugs. While the consideration of the *ranks* of each molecule in

the docking calculation against the β_2AR$^{\text{inactive}}$ was not essential, comparison of the *poses* oftentimes helped

in deciding whether or not a particular molecule was likely an agonist or not. The specific conformations

elucidated in the crystallographically determined receptor structures appear to be sufficient to enrich agonists,

i.e. that "function follows form". Our study also demonstrated that information is added with new structures

and that a dual reranking considering ranking lists of docking calculations to β_2AR$^{\text{active}}$ leads to the largest

number of agonists.

Last, but not least, we identified novel agonists for the β_2AR featuring a previously undescribed pyrazole

moiety and intrinsic efficacies on par with clinically used drugs. Several derivatives were explored during

this project, revealing insights into their SAR. Docking calculations thus once again yielded a novel chemo-

type, (Sabio et al., 2008; Kolb et al., 2009; Weiss et al., 2013; Schmidt et al., 2017) particularly remarkable

for a target as well-explored as the β_2AR.

While our findings should be readily transferable to other class A GPCRs with similarly successful results,

this approach could at the moment be more difficult when targeting GPCRs from other classes due to the

smaller number of available crystal structures. Yet, with structures appearing at the rate that they currently

do, this is an issue that will rapidly disappear in the future.

Acknowledgements

We thank Florent Chevillard for contributing the prepared structure of PDB 4LDL and PDB 2RH1 and the script for similarity searches based on the Tanimoto coefficient. Niek van Hilten contributed the method and the script for selective reranking. We thank Richard Proudman for technical help, especially with cell culture. We also want to acknowledge Felix Terwesten, Corey Taylor and Tobias Hüfner for maintaining the computer network and software environment used in this study.

Authorship contributions

Participated in research design: Scharf, and Kolb.

Conducted experiments: Scharf, and Baker.

Performed data analysis: Scharf, Baker, and Kolb.

Wrote or contributed to writing of manuscript: Scharf, Bünemann, Baker, and Kolb.

References

Baker JG (2005) Site of action of β-ligands at the human β1-adrenoceptor. *J Pharmacol Exp Ther* **313**:1163–1171.

Baker JG (2005) The selectivity of β-adrenoceptor antagonists at the human β1, β2 and β3 adrenoceptors. *Br J Pharmacol* **144**:317–322.

Baker JG (2010) The selectivity of β-adrenoceptor agonists at human β_1-, β_2- and β_3-adrenoceptors. *Br J Pharmacol* **160**:1048–1061.

Baker JG, Hall IP, and Hill SJ (2004) Temporal characteristics of cAMP response element-mediated gene transcription: Requirement for sustained cAMP production. *Mol Pharmacol* **65**:986–998.

Baker JG, Proudman RGW, and Hill SJ (2014) Identification of key residues in transmembrane 4 responsible for the secondary, low-affinity conformation of the human β1-adrenoceptor. *Mol Pharmacol* **85**:811–829.

Ballesteros JA and Weinstein H (1995) Integrated methods for the construction of three-dimensional models and computational probing of structure-function relations in G protein-coupled receptors. In Sealfon SC, ed., *Receptor Molecular Biology*, vol. 25 of *Methods in Neurosciences*, chap. 19, pp. 366–428. Academic Press, San Diego, CA.

Carlsson J, Coleman RG, Setola V, Irwin JJ, Fan H, Schlessinger A, Sali A, Roth BL, and Shoichet BK (2011) Ligand discovery from a dopamine D(3) receptor homology model and crystal structure. *Nat Chem Biol* **7**:769–778.

Cherezov V, Rosenbaum DM, Hanson MA, Rasmussen SGF, Thian FS, Kobilka TS, Choi HJ, Kuhn P, Weis WI, Kobilka BK, and Stevens RC (2007) High-resolution crystal structure of an engineered human β_2-adrenergic G protein-coupled receptor. *Science* **318**:1258–1265.

Chevillard F, Stotani S, Karawajczyk A, Hristeva S, Pardon E, Steyaert J, Tzalis D, and Kolb P (2019) Interrogating dense ligand chemical space with a forward-synthetic library. *Proc Natl Acad Sci U S A* **116**:11496–11501.

De Lean A, Stadel JM, and Lefkowitz RJ (1980) A ternary complex model explains the agonist-specific binding properties of the adenylate cyclase-coupled β-adrenergic receptor. *J Biol Chem* **255**:7108–7117.

Gaulton A, Bellis LJ, Bento AP, Chambers J, Davies M, Hersey A, Light Y, McGlinchey S, Michalovich D, Al-Lazikani B, and Overington JP (2012) ChEMBL: a large-scale bioactivity database for drug discovery. *Nucleic Acids Res* **40**:D1100–D1107.

Granneman JG (2001) The putative β_4-adrenergic receptor is a novel state of the β_1-adrenergic receptor. *Am J Physiol Endocrinol Metab* **280**:E199–E202.

Irwin JJ, Sterling T, Mysinger MM, Bolstad ES, and Coleman RG (2012) ZINC: A free tool to discover chemistry for biology. *J Chem Inf Model* **52**:1757–1768.

Kolb P, Phan K, Gao ZG, Marko AC, Šali A, and Jacobson KA (2012) Limits of ligand selectivity from docking to models: In silico screening for A_1 adenosine receptor antagonists. *PLOS ONE* **7**:e49910.

Kolb P, Rosenbaum DM, Irwin JJ, Fung JJ, Kobilka BK, and Shoichet BK (2009) Structure-based discovery of β_2-adrenergic receptor ligands. *Proc Natl Acad Sci U S A* **106**:6843–6848.

Konkar AA, Zhu Z, and Granneman JG (2000) Aryloxypropanolamine and catecholamine ligand interactions with the β1-adrenergic receptor: Evidence for interaction with distinct conformations of β1-adrenergic receptors. *J Pharmacol Exp Ther* **294**:923–932.

Kruse AC, Weiss DR, Rossi M, Hu J, Hu K, Eitel K, Gmeiner P, Wess J, Kobilka BK, and Shoichet BK (2013) Muscarinic receptors as model targets and antitargets for structure-based ligand discovery. *Mol Pharmacol* **84**:528–540.

Kuntz ID, Meng EC, Oatley SJ, Langridge R, and Ferrin TE (1982) A geometric approach to macromolecule-ligand interactions. *J Mol Biol* **161**:269–288.

Latorraca NR, Venkatakrishnan AJ, and Dror RO (2017) GPCR dynamics: Structures in motion. *Chem Rev* **117**:139–155.

Meng EC, Shoichet BK, and Kuntz ID (1992) Automated docking with grid-based energy evaluation. *J Comput Chem* **13**:505–524.

Momany FA and Rone R (1992) Validation of the general purpose QUANTA 3.2/CHARMm force field. *J Comput Chem* **13**:888–900.

Mysinger MM, Carchia M, Irwin JJ, and Shoichet BK (2012) Directory of useful decoys, enhanced (DUD-E): better ligands and decoys for better benchmarking. *J Med Chem* **55**:6582–6594.

Mysinger MM and Shoichet BK (2010) Rapid context-dependent ligand desolvation in molecular docking. *J Chem Inf Model* **50**:1561–1573.

Pardon E, Betti C, Laeremans T, Chevillard F, Guillemyn K, Kolb P, Ballet S, and Steyaert J (2018) Nanobody-enabled reverse pharmacology on GPCRs. *Angew Chem Int Ed* **57**:5292–5295.

Rasmussen SG, Choi HJ, Fung JJ, Pardon E, Casarosa P, Chae PS, DeVree BT, Rosenbaum DM, Thian FS, Kobilka TS, Schnapp A, Konetzki I, K SR, Gellman S, Pautsch A, Steyaert J, Weis W, and Kobilka BK (2011) Structure of a nanobody-stabilized active state of the beta(2) adrenoceptor. *Nature* **469**:175–180.

Rasmussen SGF, DeVree BT, Zou Y, Kruse AC, Chung KY, Kobilka TS, Thian FS, Chae PS, Pardon E, Calinski D, Mathiesen JM, Shah STA, Lyons JA, Caffrey M, Gellman SH, Steyaert J, Skiniotis G, Weis WI, Sunahara RK, and Kobilka BK (2011) Crystal structure of the beta(2) adrenergic receptor-Gs protein complex. *Nature* **477**:549–U311.

Ring AM, Manglik A, Kruse AC, Enos MD, Weis WI, Garcia KC, and Kobilka BK (2013) Adrenaline-activated structure of β2-adrenoceptor stabilized by an engineered nanobody. *Nature* **502**:575–579.

Sabio M, Jones K, and Topiol S (2008) Use of the X-ray structure of the β_2-adrenergic receptor for drug discovery. Part 2: Identification of active compounds. *Bioorg Med Chem Lett* **18**:5391–5395.

Schmidt D, Bernat V, Brox R, Tschammer N, and Kolb P (2015) Identifying modulators of CXC receptors 3 and 4 with tailored selectivity using multi-target docking. *ACS Chem Biol* **10**:715–724.

Schmidt D, Gunera J, Baker JG, and Kolb P (2017) Similarity- and substructure-based development of
β_2-adrenergic receptor ligands based on unusual scaffolds. *ACS Med Chem Lett* **8**:481–485.

Shoichet BK and Kuntz ID (1993) Matching chemistry and shape in molecular docking. *Protein Eng* **6**:723–
732.

Shoichet BK, Leach AR, and Kuntz ID (1999) Ligand solvation in molecular docking. *Proteins: Struct,
Funct, Bioinf* **34**:4–16.

Sterling T and Irwin JJ (2015) ZINC 15 - ligand discovery for everyone. *J Chem Inf Model* **55**:2324–2337.

Wacker D, Fenalti G, Brown MA, Katritch V, Abagyan R, Cherezov V, and Stevens RC (2010) Conserved
binding mode of human β_2 adrenergic receptor inverse agonists and antagonist revealed by X-ray crystal-
lography. *J Am Chem Soc* **132**:11443–11445.

Wawer M and Bajorath J (2010) Similarity-potency trees: A method to search for SAR information in
compound data sets and derive sar rules. *J Chem Inf Model* **50**:1395–1409.

Weiss DR, Ahn S, Sassano MF, Kleist A, Zhu X, Strachan R, Roth BL, Lefkowitz RJ, and Shoichet BK
(2013) Conformation guides molecular efficacy in docking screens of activated β-2 adrenergic G protein
coupled receptor. *ACS Chem Biol* **8**:1018–1026.

Zheng Z, Huang XP, Mangano TJ, Zou R, Chen X, Zaidi SA, Roth BL, Stevens RC, and Katritch V (2017)
Structure-based discovery of new antagonist and biased agonist chemotypes for the kappa opioid receptor.
J Med Chem **60**:3070–3081.

Footnotes

Legends for Figures

Figure 1: Schematic representation of the docking calculations of molecules to the β_2AR^{active} (PDB IDs 4LDL, 3SN6) and the $\beta_2AR^{inactive}$ (PDB IDs 3NY9, 2RH1) and the obtained four different ranking lists of molecules. The IDs of the selected molecules are given and marked in white text if found to be agonists whereas those with names in black text did not interact with either the β_2AR or the β_1AR. No antagonists (i.e. molecules that bind to the receptor but do not stimulate a response) were identified.

Figure 2: Dose-response curves for competition binding and functional assay results for compound **1**. (A,B) Whole cell competition binding with ^{3}H-CGP 12177 in (A) CHO-β_1AR cells and (B) CHO-β_2AR cells. Bars represent total and non-specific binding. Concentration of the radioligand was 0.77 nM for both experiments. (C,D) CRE-SPAP production in (C) CHO-β_1AR cells in response to **1** in the presence and absence of CGP 20712A and in (D) CHO-β_2AR cells in response to **1** in the presence and absence of ICI 118551. Bars represent basal CRE-SPAP production or production in response to 10 μM isoprenaline or (C) 10 nM CGP 20712A or (D) 3 nM ICI 118551. (A-D) Data points are mean $\pm$ sem of triplicates and the experiments are representative for (A) 5, (B) 5, (C) 8 and (D) 7 seperate experiments.
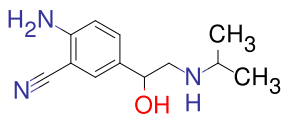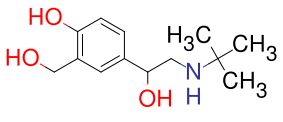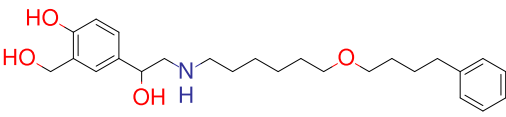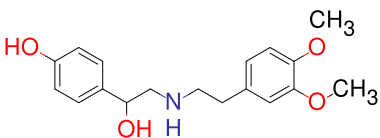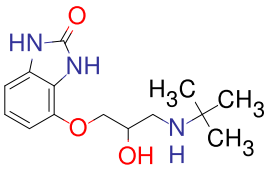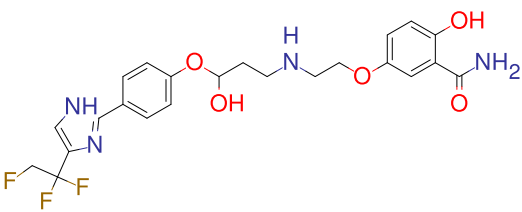
Figure 3: ROC plots of known ligand and decoy docking calculations after (A) dual reranking of the ranking lists of the docking calculations to β_2AR^{active} 3SN6 and 4LDL and (B) after selective reranking of the ranking lists of the docking calculations to β_2AR^{active} 3SN6 vs. $\beta_2AR^{inactive}$ 3NY9. Enrichment of known actives over decoys was calculated treating only antagonists (blue curve), only agonists (orange curve) or all ligands (green curve) as actives. Numbers represent the area under the curve and the dotted line indicates random enrichment.

Figure 4: (A) Molecule pose of **1** from the docking calculation to the β_2AR^{active} structure 3SN6. The molecule forms interactions with residues D113$^{3.32}$ and N312$^{7.39}$. (B) Molecule pose of **8** from the docking calculation to the $\beta_2AR^{inactive}$ structure 2RH1. The molecule is interacting with D113$^{3.32}$, probably also with N293$^{6.55}$ and N312$^{7.39}$. It stretches up towards ECL2 and is too bulky to fit into the smaller cavity of the β_2AR^{active}.

Figure 5: Overlay of the β_2AR structures used in this work as prepared for the docking calculations. Two structures in active conformations (3SN6 [orange] and 4LDL [magenta]) and two structures in inactive conformations (3NY9 [cyan] and 2RH1 [green]) are compared. Differences of side chain positions between all structures as well as between active conformations and inactive conformations can be observed. Although these changes can be considered small, they still allow to distinguish agonists and antagonists in docking calculations. (A) Side view of the orthosteric binding pocket. Residues that are involved in ligand binding are highlighted (compare also Fig. 4). (B) Top view from the extracellular side of the receptor into the orthosteric binding pocket. The same residues as in (A) are highlighted as sticks as well as residue Y308$^{7.35}$, which was not shown in (A) for clarity. Other residues are shown in line representation in this panel to give a better impression of overall differences of the side chain positions in the binding pocket.

Tables

Table 1: $\log K_D$ values (affinity) of known and novel compounds detected through docking to the β_2AR structures in active and inactive conformations, as determined from ^{3}H-CGP 12177 whole cell binding (mean $\pm$SEM of n separate experiments). Compounds are in order of efficacy ratio at the β_2AR (a measure of intrinsic efficacy, see text and Table 2).

Compound	Structure	β_1AR $\log K_D$	n	β_2AR $\log K_D$	n
Literature known reference compounds.					
Cimaterol		-6.4±0.1	3	-7.1±0.1	3
Salbutamol		-5.0±0.1	5	-6.3±0.1	5
Salmeterol		-5.7±0.0	7	-9.1±0.0	7
Denopamine		-6.0±0.1	5	-5.3±0.1	5
CGP 12177		-9.4±0.0	3	-9.6±0.1	3
CGP 20712A		-8.6±0.2	6	-5.8±0.1	8
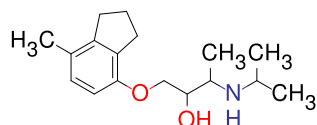
ICI 118551		-6.8±0.1	7	-9.3±0.1	7

Compounds chosen from docking calculations.
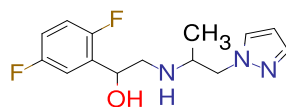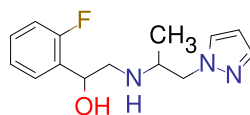
1		-6.3±0.0	5	-6.3±0.1	5
2		-6.0±0.0	5	-5.9±0.1	5
3		-5.0±0.1	5	-5.6±0.0	5
4		-5.5±0.1	5	-5.9±0.1	5
5		-5.6±0.0	5	-5.4±0.1	5
6		-5.8±0.0	6	-5.7±0.0	5
7		-5.8±0.0	5	-5.9±0.0	5
8		-5.0±0.0	6	-6.1±0.1	6
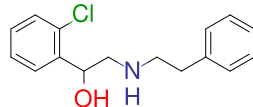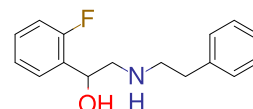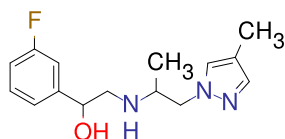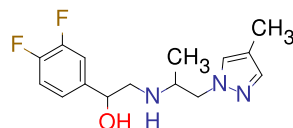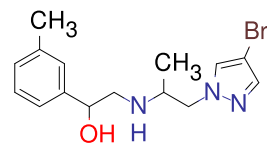
9		-5.0±0.1	5	$IC_{50} > -4$	5
10		no binding	5	$IC_{50} > -4$	5
11[a]		-5.3±0.0	5	-5.3±0.0	5
12[a]		-6.2±0.0	6	-6.1±0.1	6
14[a]		$IC_{50} > -4$	6	$IC_{50} > -4$	6
22		$IC_{50} > -4$	5	$IC_{50} > -4$	6
25		no binding	5	$IC_{50} > -4$	5
26		no binding	5	$IC_{50} > -4$	5
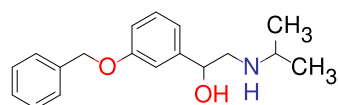
a Molecules selected from secondary screen.

Table 2: Agonist response to compounds as determined from CRE-SPAP gene transcription in CHO-β_1 and CHO-β_2 cells given as log EC_{50} values and % 10 μM isoprenaline responses in n separate experiments. Agonist responses were also examined in the presence of CGP 20712A (β_1AR) or ICI 118551 (β_2AR) and where a parallel shift was achieved, a log K_D value for the antagonist is also given.

Compound	β_1AR					β_2AR					log(efficacy ratio)	
	log EC_{50}	% isop	n	log K_D CGP 20712A	n	log EC_{50}	% isop	n	log K_D ICI 118551	n	β_1AR	β_2AR
Literature known reference compounds.												
Cimaterol	-8.6±0.1	100±9	12	-9.0±0.1	20	-9.7±0.1	98±6	12	-9.7±0.1	23	2.21	2.59
Salbutamol	-6.5±0.2	109±9	7	-9.0±0.2	6	-8.6±0.1	95±6	6	-9.8±0.1	7	1.55	2.39
Salmeterol	-6.8±0.1	110±9	7	-8.9±0.3	4	-10.9±0.2	100±7	8	-9.1±0.0	6	1.02	1.81
Denopamine	-8.1±0.1	101±4	7	-9.2±0.3	4	-6.4±0.1	65±6	7	-9.6±0.1	4	2.13	1.02
CGP 12177	-8.5±0.1	82±7	13	-7.0±0.1	7	-9.7±0.1	37±4	10	-9.6±0.1	14	-0.92	0.16

Table is continued on the following page.

Continuation of Table 2

Compounds chosen from docking calculations.

Compound	β$_1$AR					β$_2$AR					log(efficacy ratio)	
	log EC_{50}	% isop	n	log K_D CGP 20712A	n	log EC_{50}	% isop	n	log K_D ICI 118551	n	β$_1$AR	β$_2$AR
1	-7.5±0.1	80±4	8	-8.6±0.1	7	-8.0±0.1	90±6	7	-9.6±0.1	6	1.2	1.76
2	-7.2±0.1	82±6	7	-8.6±0.2	5	-7.5±0.1	97±4	7	-9.5±0.1	6	1.22	1.64
3	-6.3±0.1	33±6	6			-7.0±0.1	95±8	6	-9.6±0.1	5	1.27	1.39
4	-6.7±0.1	60±6	7			-7.1±0.1	79±4	7	-9.5±0.1	6	1.25	1.24
11[a]	-6.6±0.1	113±7	6	-9.4±0.3	3	-6.5±0.1	92±9	6	-9.7±0.2	5	1.35	1.23
5	-7.0±0.2	85±7	6	-9.1±0.3	4	-6.5±0.1	86±11	6	-9.6±0.1	5	1.42	1.19
12[a]	-7.3±0.1	78±6	7	-9.3±0.1	5	-7.2±0.1	96±9	6	-9.7±0.1	6	1.10	1.05
6	-6.8±0.1	82±9	6	-9.0±0.2	3	-6.6±0.1	75±8	6	-9.8±0.1	5	0.92	0.89
7	-6.9±0.0	90±5	6	-9.1±0.2	3	-6.6±0.1	86±6	7	-9.6±0.1	6	1.09	0.73
8	10 μM = 21±7		8			-6.2±0.1	35±7	6				
9	10 μM = 30±12		7			10 μM = 29±4		7				
10	no response		6			10 μM = 50±8		7				

[a] Molecules selected from secondary screen.

No response was seen for CGP 20712A, ICI 118551 nor the docking screen compounds **13**[a], **14**[a], **15**[a], **16**, **17**, **18**, **19**, **20**, **21**, **22**, **23**, **24**, **25**,

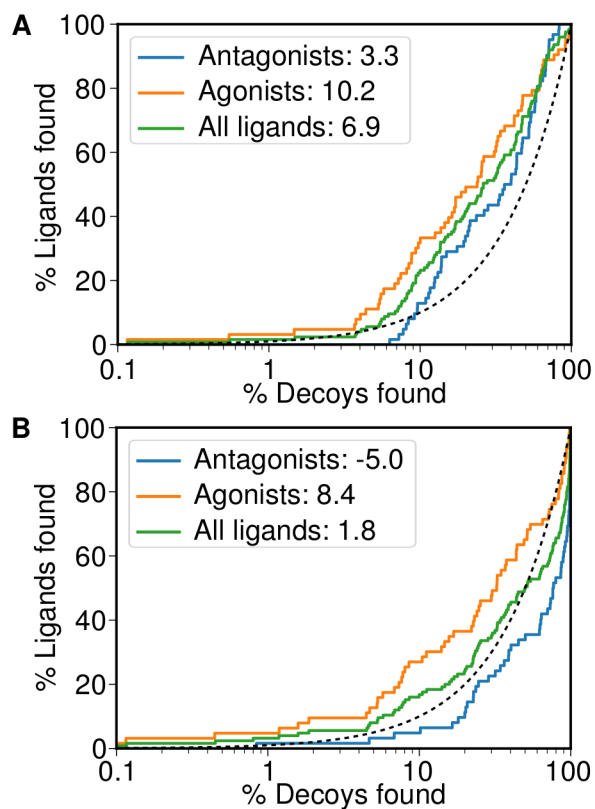**26**, **27** (n=5 for each ligand at each receptor).
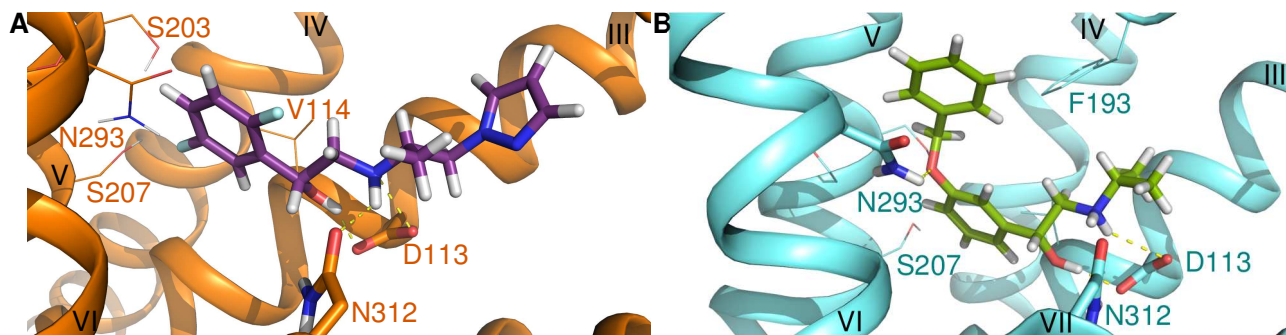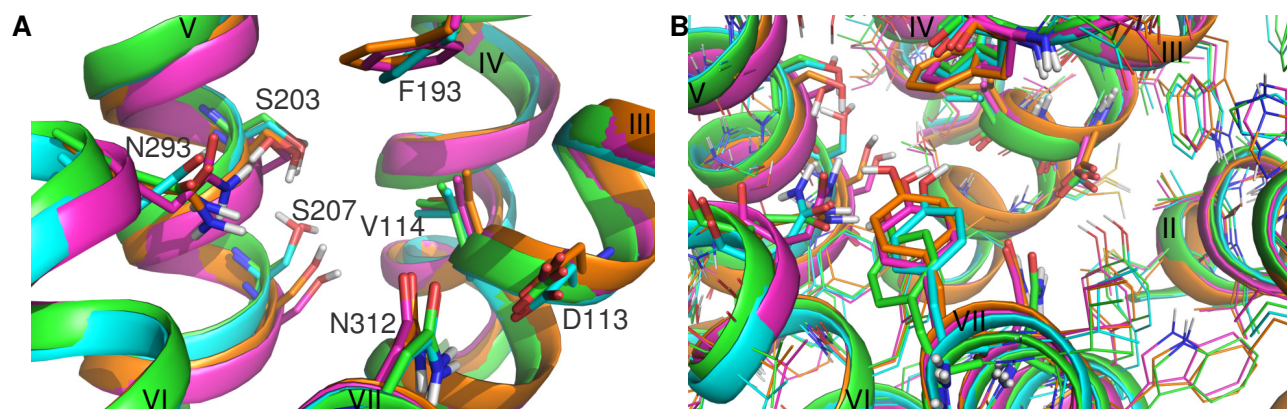
Figures

Figure 1
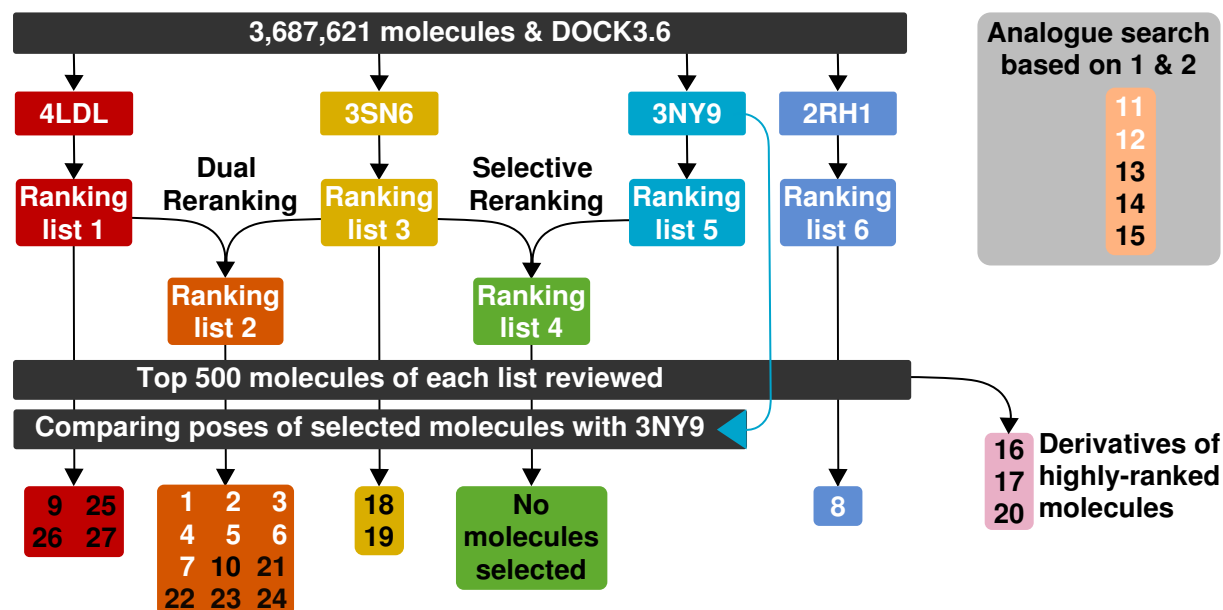
Figure 2
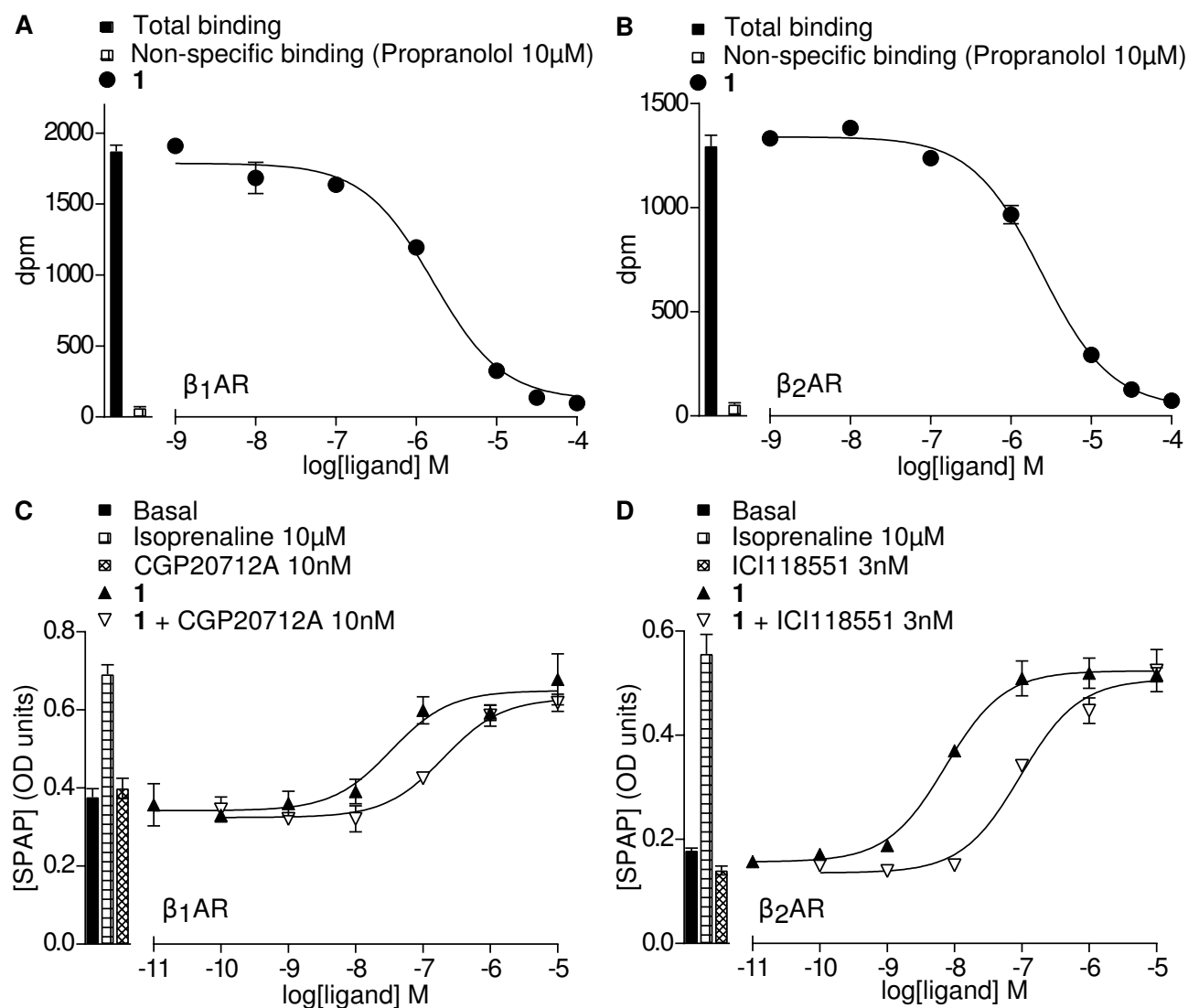
Figure 3

Figure 4

Figure 5

MOL # 117515

Comparative docking to distinct G protein-coupled receptor conformations exclusively yields ligands with agonist efficacy

Journal: Molecular Pharmacology

Magdalena M. Scharf[a], Moritz Bünemann[b], Jillian G. Baker[c], and Peter Kolb[a,*]

[a]Institute of Pharmaceutical Chemistry, Philipps-University Marburg, Marbacher Weg 6, 35032 Marburg, Germany

[b]Institute of Pharmacology and Clinical Pharmacy, Philipps-University Marburg, Karl-von-Frisch-Straße 2, 35043 Marburg, Germany

[c]Cell Signalling, School of Life Science, Queen's Medical Center, University of Nottingham, Nottingham NG7 2UH, UK

Supplemental Data

Supplemental assay: Preliminary cAMP accumulation assay

Supplemental Method For a preliminary screen for agonistic activity of the selected compounds, the G_S assay kit from *Cisbio* was used. HEK293T cells expressing the β_2AR endogenously were grown in Dulbecco's modified Eagle's medium (DMEM) containing 10% fetal bovine serum, 2 mM L-glutamine, 100 U/mL Penicillin and 100 µg/mL Streptomycin at 37°C and 5% CO_2.

The assay protocol provided by *Cisbio* was optimised to yield the optimal assay window for the used system. Cells were suspended in modified tyrode buffer (10 mM HEPES, 1 mM $CaCl_2$, 0.5 mM $MgCl_2$, 4.2 mM KCl, 146 mM NaCl, 5.5 mM Glucose; pH=7.4) supplemented with 0.5 mM IBMX at a concentration of 1400 cells/µL and 5 µL cell suspension transferred to the wells of a 384-well plate.

To measure agonism, 5 µL buffer or compound dilution in buffer (two times the final concentration) were added to each well and incubated at room temperature for 10 min. Detection reagents were added as recommended by *Cisbio* (5 µL per well of one time dilution detection reagent in the provided lysis buffer). The plates were then incubated for 1 h at room temperature in the dark, before they were read on a *Tecan Spark 20M* plate reader. Isoprenaline dose-response curves were included in each measurement as a reference as well as measurements to account for basal activity and background fluorescence of the detection reagents.

To determine antagonism, the protocol was varied slightly. To each well containing the cell suspension, 3 µL buffer or compound dilution in buffer (3.3 times the final concentration) were added and incubated at room temperature for 10 min. After this incubation, 2 µL buffer or isoprenaline (final concentration in the well: 80 nM) were added and the plate was incubated for another 10 min at room temperature. Detection reagents were then added as recommended by *Cisbio* and the plates were incubated at room temperature in the dark for 1 h. After 1 h, the plate was read on a *Tecan Spark 20M* plate reader. Propranolol was used as a reference compound in each measurement and results were adjusted for basal activity and background fluorescence of the detection reagents. The resulting data was analysed as described in the *Cisbio* assay protocol and plotted using GraphPad Prism 7.

Supplemental Results Although the assay showed only low sensitivity and could therefore not be used to determine reliable EC_{50} values, it was used to gather qualitative information. The two ligands with the

highest efficacy ratio towards the β_2AR, **1** and **2**, were identified as agonists with this assay (see Supplemental Figure 1). All of the other agonists that were identified in the CRE-SPAP assays showed increased HTRF ratios for the higher concentrations in the antagonist assay setup.

Supplemental Figures
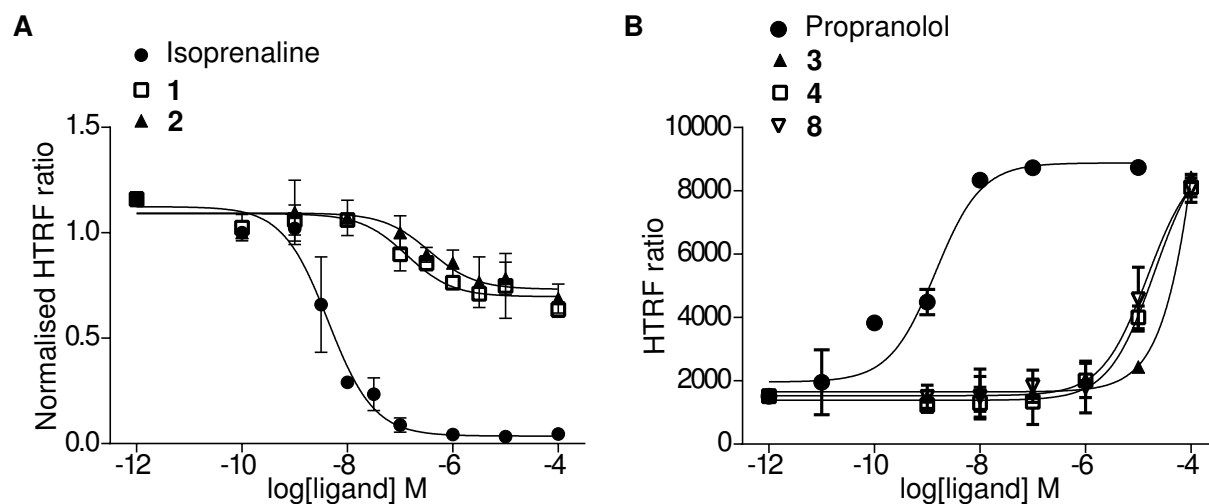
Supplemental Figure 1: Dose-response curves of some of the tested compounds in a preliminary cAMP accumulation assay. (A) Compounds **1** and **2** showed agonistic activity in the assay. Responses were normalised to the maximum response of Isoprenaline. (B) Compounds **4**, **3** and **8** showed increasing HTRF ratios for higher concentrations in the antagonist assay setup. Propranolol was measured as a reference compound. Data points are mean $\pm$ sem of duplicates in (A) 2 and (B) 1 seperate experiment.
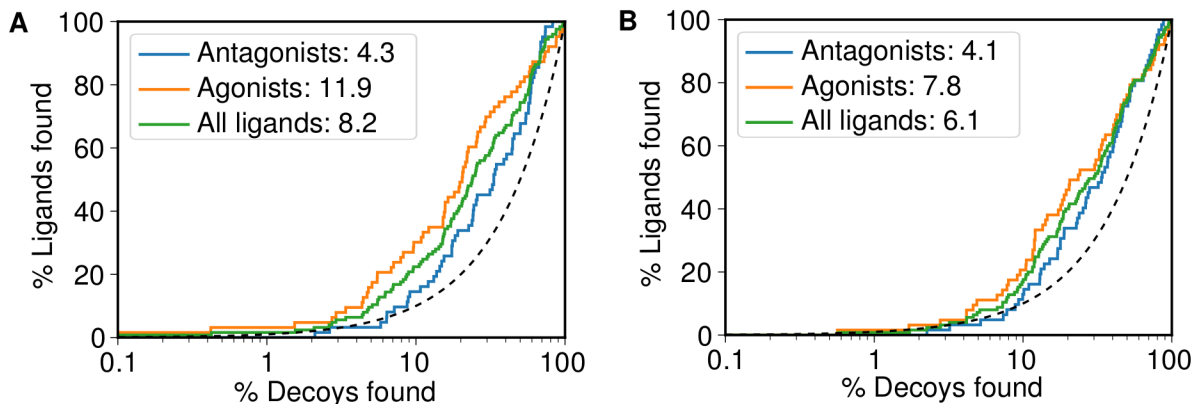
Supplemental Figure 2: ROC plots of known ligand and decoy docking calculations to β_2AR^{active} (A) 3SN6 and (B) 4LDL. Enrichments were calculated using only antagonists (blue curve), only agonists (orange curve) or all ligands (green curve) as actives. Numbers are area under the curve and the dotted line represents random enrichment.

Supplemental Tables

Supplemental Table 1: SMILES and vendor information of all tested molecules.

Mol	SMILES string	Vendor	Vendor ID	ZINC ID
1	CC(Cn1cccn1)[NH2+]CC(c2cc(ccc2F)F)O	Enamine[a]	Z1139549933	C49075870
2	CC(Cn1cccn1)[NH2+]CC(c2ccccc2F)O	Enamine[a]	Z1139549920	C49075832
3	c1ccc(cc1)CC[NH2+]CC(c2ccccc2Cl)O	Enamine[a]	BBV-32195129	C32122137
4	c1ccc(cc1)CC[NH2+]CC(c2ccccc2F)O	Enamine[a]	BBV-32188060	C32110999
5	Cc1cnn(c1)CC(C)[NH2+]CC(c2cccc(c2)F)O	Enamine[a]	Z1139457046	C69489460
6	Cc1cnn(c1)CC(C)[NH2+]CC(c2ccc(c(c2)F)F)O	Enamine[a]	Z1139457054	C69534697
7	Cc1cccc(c1)C(C[NH2+]C(C)Cn2cc(cn2)Br)O	Enamine[a]	Z1582993358	C90520132
8	CC(C)[NH2+]CC(c1cccc(c1)OCc2ccccc2)O	Enamine[a]	Z1597907783	C32131959
9	Cc1c(c(n(n1)CC[NH2+]C(C)Cc2ccccc2F)C)Cl	ChemBridge[d]	75024249	C65461465
10	COc1cccc(c1)C(C[NH2+]C2Cc3cccc(c3OC2)OC)O	Enamine[a]	Z1823958433	C97105309
11	CC(NCC](O)c1ccccc1F)C(C)n1cccn1	Enamine[a]	Z1143054162	C72269793

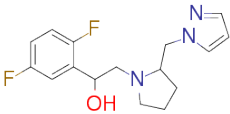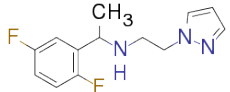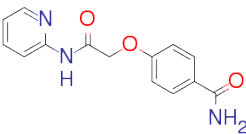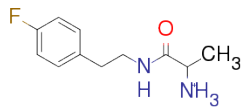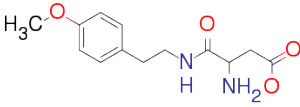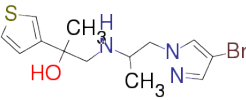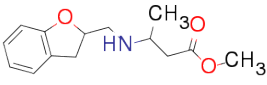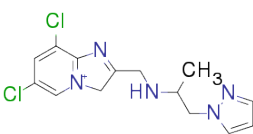| 12 | CC(Cn1cccn1)NCC(O)c1ccc(F)c(F)c1 | Enamine[a] | Z1139549938 | C49075899 |
13	OC(CN1CCCC1Cn1cccn1)c1cc(F)ccc1F	Enamine[a]	Z1139479667	C71875670
14	CC(Cn1cccn1)NCCOc1ccccc1F	Enamine[a]	Z414797082	C69387511
15	CC(NCCn1cccn1)c1cc(F)ccc1F	Enamine[a]	Z1139746195	C42538939
16	c1ccnc(c1)NC(=O)COc2ccc(cc2)C(=O)N	Enamine[a]	Z848936154	C49105831
17	CC(C(=O)NCCc1ccc(cc1)F)[NH3+]	FCH Group[b]	FCG1450162145	C19502698
18	c1ccc2c(c1)nc(o2)C[NH2+]C3CCCN(C3)c4cccnn4	Enamine[a]	Z1139245547	C69872322
19	COc1ccc(cc1)CCNC(=O)C(CC(=O)[O-])[NH3+]	Enamine[a]	BBV-39452572	C83483625
20	CC(Cn1cc(cn1)Br)[NH2+]CC(C)(c2ccsc2)O	Enamine[a]	Z1441405249	C95968346
21	CC(CC(=O)OC)[NH2+]CC1Cc2ccccc2O1	Enamine[a]	BBV-32282913	C38009848
22	c1cc(cnc1)c2c(c[nH]n2)C[NH2+]Cc3cc4cc(ccc4s3)F	Enamine[a]	Z2241129897	C65595055
23	CC(Cn1cccn1)[NH2+]Cc2cn3cc(cc(c3n2)Cl)Cl	Enamine[a]	Z1139744745	C69389875
24	c1cc(cnc1)c2c(c[nH]n2)CNCc3ccc(nc3)n4ccnc4	Enamine[a]	Z2241113193	C97159292
25	c1cc(ccc1C[NH2+]Cc2c[nH]nc2c3ccc(cc3)F)n4cncn4	UORSY[c]	PB1135242967	C78552850
26	Cc1ccc(o1)c2c(c[nH]n2)C[NH2+]Cc3cn4cc(ccc4n3)Cl	Enamine[a]	Z2241115638	C97159595
27	CC(C(=O)Nc1ccc(c(c1)C(F)(F)F)Cl)[NH2+]C	Enamine[a]	Z44508089	C55421527
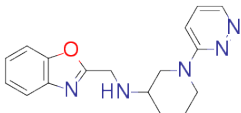
a SIA Enamine, Vestienas iela 2B, LV-1035 Riga, LATVIA

b FCH Group, PO Box 438, 14017 Chernigiv, UKRAINE

c Ukrorgsyntez Ltd., PO Box 59, 02002 Kyiv, UKRAINE

d ChemBridge Corporation, 11199 Sorrento Valley Rd., Suite 206, San Diego, CA 92121, USA

Supplemental Table 2: Compounds selected from the docking calculations that did not show affinity to either the β₁AR or the β₂AR. These molecules did not induce agonist activity, either.

Mol	Structure	β₁AR $log K_D$	n	β₂AR $log K_D$	n
13[a]		no binding	5	no binding	5
15[a]*		no binding	5	no binding	5
16		no binding	5	no binding	5
17		no binding	5	no binding	5
18		no binding	5	no binding	5
19		no binding	5	no binding	5
20		no binding	5	no binding	5
21		no binding	5	no binding	5
23		no binding	5	no binding	5

| **24** | | no binding | 5 | no binding | 5 |

| **27** | | no binding | 5 | no binding | 5 |

a Molecules chosen from secondary screen.

Supplemental Table 3: Similarity of tested molecules to ligands of the β_2AR in ChEMBL bioactivity dataset. ChEMBL ID and Smiles of most similar molecule as well as Tanimoto ECFP4 coefficient are listed (first entry of the result table if several molecules with the same smilarity were found).

Mol	ChEMBL ID	Smiles	Tanimoto
1	CHEMBL16476	CC(C)NCC(O)c1ccc2ccccc2c1	0.25
2	CHEMBL1902627	CC(C)NCC(O)c1ccccc1Cl	0.31
3	CHEMBL599896	Cl.CC(CCc1ccccc1)NCC(O)c2cccc(c2)[N+](=O)[O-]	0.41
4	CHEMBL599896	Cl.CC(CCc1ccccc1)NCC(O)c2cccc(c2)[N+](=O)[O-]	0.41
5	CHEMBL327122	CC(C)NCC(O)c1cccc(O)c1	0.32
6	CHEMBL321468	CC(C)NCC(O)c1ccc(O)c(CO)c1	0.28
7	CHEMBL327122	CC(C)NCC(O)c1cccc(O)c1	0.32
8	CHEMBL599896	Cl.CC(CCc1ccccc1)NCC(O)c2cccc(c2)[N+](=O)[O-]	0.47
9	CHEMBL1159723	CCCc1ccccc1OCC(O)CNC(C)C	0.26
10	CHEMBL26183	COc1cccc2c(C[C@@H](C)NC[C@H](O)c3cccc(Cl)c3)c[nH]c12	0.36
11	CHEMBL1902627	CC(C)NCC(O)c1ccccc1Cl	0.45
12	CHEMBL16476	CC(C)NCC(O)c1ccc2ccccc2c1	0.39
13	CHEMBL1723653	Cc1ncc(CN2CCCC(C2)C(=O)Nc3ccc(cc3)c4cccc(F)c4)s1	0.24
14	CHEMBL1626224	CC(O)CNCCOc1ccccc1c2ccccc2	0.38
15	CHEMBL16476	CC(C)NCC(O)c1ccc2ccccc2c1	0.24

16	CHEMBL1577023	Cc1ccc(OCC(=O)Nc2ccc(cc2)c3oc4cccnc4n3)cc1	0.39
17	CHEMBL24	CC(C)NCC(O)COc1ccc(CC(=O)N)cc1	0.31
18	CHEMBL2441621	C1CN(CCN1)c2ccnc3ccccc23	0.30
19	CHEMBL3099658	COc1ccc(CCNC[C@@H](O)c2cc(O)cc(O)c2)cc1	0.37
20	CHEMBL1159717	CC(C)(C)NCC(O)c1ccccc1Cl	0.18
21	CHEMBL1200586	Cl.CCCNC(C)C(=O)Nc1ccccc1C	0.28
22	CHEMBL1573444	CN(Cc1ccccc1F)c2nc(nc3ccccc23)c4cccnc4	0.31
23	CHEMBL531401	CC(Oc1ccc(Cl)cc1Cl)c2onc(n2)c3ccc(NC(=O)c4occc4)cc3	0.21
24	CHEMBL3099899	COc1ccc(CNC(=O)c2cc(cnc2c3cccnc3)c4cc(Cl)cc(Cl)c4)cc1OC	0.30
25	CHEMBL305558	O[C@@H](CNCCc1ccc(NS(=O)(=O)c2ccc(cc2)n3ncc(n3) c4ccc(F)cc4)cc1)c5cccnc5	0.33
26	CHEMBL252766	CSc1ccc2nc(cn2c1)c3ccc(cc3)N(C)C	0.27
27	CHEMBL1439691	CCN(CC)S(=O)(=O)c1cc(NC(=O)C2=COCCO2)ccc1Cl	0.26

Supplemental Table 4: Similarity of tested molecules to ligands of any adrenergic receptor in the ChEMBL bioactivity dataset. ChEMBL ID and smiles of most similar molecule as well as Tanimoto ECFP4 coefficient are listed (first entry of the result table if several molecules with the same smilarity were found).

Mol	ChEMBL ID	Smiles	Tanimoto
1	CHEMBL15303	CC(C)NCC(O)COc1ccccc1Cn2cccn2	0.33
2	CHEMBL15303	CC(C)NCC(O)COc1ccccc1Cn2cccn2	0.42
3	CHEMBL599896	Cl.CC(CCc1ccccc1)NCC(O)c2cccc(c2)[N+](=O)[O-]	0.41
4	CHEMBL7156	OC(CNCCNC(=O)Cc1ccccc1)COC(=O)c2ccccc2F	0.42
5	CHEMBL327122	CC(C)NCC(O)c1cccc(O)c1	0.32
6	CHEMBL62072	CNCC(O)c1ccc(F)c(O)c1	0.31
7	CHEMBL25724	CC(Cc1c[nH]c2cc(C)ccc12)NCC(O)c3cccc(Cl)c3	0.32
8	CHEMBL599896	Cl.CC(CCc1ccccc1)NCC(O)c2cccc(c2)[N+](=O)[O-]	0.47

9	CHEMBL3588911	CC(C)NCc1nccn1Cc2ccccc2C	0.30
10	CHEMBL2153551	Cl.COc1cccc(OC)c1OCCNC[C@H]2COc3cccc(O)c3O2	0.36
11	CHEMBL1902627	CC(C)NCC(O)c1ccccc1Cl	0.45
12	CHEMBL16476	CC(C)NCC(O)c1ccc2ccccc2c1	0.39
13	CHEMBL1767149	CN1CCC[C@@H]1CN2N=C(Cc3ccc(F)c(F)c3)c4ccccc4C2=O	0.33
14	CHEMBL15303	CC(C)NCC(O)COc1ccccc1Cn2cccn2	0.49
15	CHEMBL15303	CC(C)NCC(O)COc1ccccc1Cn2cccn2	0.34
16	CHEMBL1577023	Cc1ccc(OCC(=O)Nc2ccc(cc2)c3oc4cccnc4n3)cc1	0.39
17	CHEMBL6863	CC(C)NCC(O)COC(=O)c1ccc(F)cc1	0.38
18	CHEMBL18772	C1CN(CCN1)c2ccc3ccccc3n2	0.31
19	CHEMBL3099658	COc1ccc(CCNC[C@@H](O)c2cc(O)cc(O)c2)cc1	0.37
20	CHEMBL371300	C[C@H](N)Cn1ncc2ccc(O)cc12	0.23
21	CHEMBL1203102	Cl.COC(=O)c1cc(ccc1O)C(O)CNCC2COc3ccccc3O2	0.31
22	CHEMBL1573444	CN(Cc1ccccc1F)c2nc(nc3ccccc23)c4cccnc4	0.31
23	CHEMBL1327	OC(Cn1ccnc1)c2ccc(Cl)cc2Cl	0.30
24	CHEMBL3588905	C(NCc1c[nH]c(n1)c2ccccc2)c3cccnc3	0.42
25	CHEMBL305558	O[C@@H](CNCCc1ccc(NS(=O)(=O)c2ccc(cc2)n3ncc(n3) c4ccc(F)cc4)cc1)c5cccnc5	0.33
26	CHEMBL351483	CC1=C(CCN2CCc3oc4ccccc4c3C2)C(=O)N5C=C(Cl)C=CC5=N1	0.30
27	CHEMBL101340	FC(F)(F)c1ccc(Cl)c(NC2=NCCN2)c1	0.31

Supplemental Data

Molecule poses from docking calculations for all tested molecules are available as PDB files in at least one of the structures 3SN6, 4LDL or 2RH1 as used for the docking calculations. A list of the PDB files can be found below sorted by compound number.

Compound 1: 3SN6_cmpd-01.pdb; 4LDL_cmpd-01.pdb

Compound 2: 3SN6_cmpd-02.pdb; 4LDL_cmpd-02.pdb

Compound 3: 3SN6_cmpd-03.pdb; 4LDL_cmpd-03.pdb

Compound 4: 3SN6_cmpd-04.pdb; 4LDL_cmpd-04.pdb

Compound 5: 3SN6_cmpd-05.pdb; 4LDL_cmpd-05.pdb

Compound 6: 3SN6_cmpd-06.pdb; 4LDL_cmpd-06.pdb

Compound 7: 3SN6_cmpd-07.pdb; 4LDL_cmpd-07.pdb

Compound 8: 2RH1_cmpd-08.pdb; 3SN6_cmpd-08.pdb; 4LDL_cmpd-08.pdb

Compound 9: 4LDL_cmpd-09.pdb

Compound 10: 3SN6_cmpd-10.pdb; 4LDL_cmpd-10.pdb

Compound 11: 3SN6_cmpd-11.pdb

Compound 12: 3SN6_cmpd-12.pdb

Compound 13: 3SN6_cmpd-13.pdb

Compound 14: 3SN6_cmpd-14.pdb

Compound 15: 3SN6_cmpd-15.pdb

Compound 16: 3SN6_cmpd-16.pdb

Compound 17: 3SN6_cmpd-17.pdb

Compound 18: 3SN6_cmpd-18.pdb

Compound 19: 3SN6_cmpd-19.pdb

Compound 20: 3SN6_cmpd-20.pdb

Compound 21: 3SN6_cmpd-21.pdb; 4LDL_cmpd-21.pdb

Compound 22: 3SN6_cmpd-22.pdb; 4LDL_cmpd-22.pdb

Compound 23: 3SN6_cmpd-23.pdb; 4LDL_cmpd-23.pdb

Compound 24: 3SN6_cmpd-24.pdb; 4LDL_cmpd-24.pdb

Compound 25: 4LDL_cmpd-25.pdb

Compound 26: 4LDL_cmpd-26.pdb

Compound 27: 4LDL_cmpd-27.pdb